Effect of *N*-methyl deuteration on pharmacokinetics and pharmacodynamics of Enzalutamide

Xuehai Pang [a,b,†], Lingling Peng [c,†] and Yuanwei Chen [a,b,c,d,*]

[a]University of Chinese Academy of Sciences, Chengdu Institute of Organic Chemistry, Chengdu, 610041, China.

[b]University of Chinese Academy of Sciences, Beijing, 100049, China.

[c]Lab of YWChen, Cancer Center, West China Hospital, Sichuan University and Collaborative Innovation Center, Chengdu, 610041, China.

[d]Hinova Pharmaceuticals Inc., Suite 301, Rongyao Building B, #5 South KeYuan Road, Chengdu 610041, China

ABSTRACT

Enzalutamide, a 2nd generation antiandrogen, has been developed for the treatment of CRPC. We synthesized the deuterated analogues **6** and found that it showed higher drug exposure and thus stronger anti-tumor potency in preclinical settings. Compound **6** is being developed clinically for the potential to be differentiated from enzalutamide through reduced dosages and a higher safety margin.

Keywords

CRPC; Enzalutamide; Deuterated drug; PK/PD; LNCaP/AR xenograft.

*Corresponding author. Tel.: +86-18602831330; fax: +86-02885058465; e-mail: ywchen@scu.edu.cn

† These authors contributed equally.

Introduction

Prostate cancer (PC) is the most common cancer in males in many developed countries, and the incidence of prostate cancer has been increasing in the developing world as well.[1] Androgens, especially testosterone (T) and dihydrotestosterone (DHT) (Figure 1, **1** and **2**), play an important role in the progression of PC through the hypothalamic-pituitary-adrenal/gonadal axis.[2-4] The androgen deprivation therapy (ADT), orchidectomy combined with antiandrogens, has significantly prolonged the survival of PC patients.[5-7] However, progression of the castration-sensitive disease eventually results in castration-resistance prostate cancer (CRPC) within 1-2 years. The tumor of CRPC regrows even in the presence of low circulating endogenous ligand (e.g. DHT), and it no longer responds to classical AR antagonists, such as bicalutamide (Figure 1, **3**).[8-12] CRPC has been indicated to associate with a number of potential mechanisms, such as AR overexpression[13-16], AR gene mutations[17,18], and androgens synthesized by the PC cells[17,19], all of which lead to AR signaling reactivation. On the other hand, some classical AR antagonists, such as **3**, can change into agonists in CRPC.[20,21]

The dependence of CRPC still on AR signaling has led to the development of two novel therapies such as abiraterone (Figure 1, **4**), a potent and selective inhibitor of CYP17A1, and enzalutamide, a 2nd generation of AR antagonist for the treatment of CRPC. Enzalutamide (Figure 1, **5**) has 5-10 fold higher affinity for AR than bicalutamide and has no AR agonist activity.[22,23] In a randomized and double-blind phase III trial in patients with mCRPC progressing after docetaxel therapy, enzalutamide significantly prolonged overall survival, and was also associated with significant benefits in health-related quality of life and in pain palliation.[24,25] However, **5** carried a potential risk of seizures that appears to be dose-dependent.[24,25]

Applying the deuterium kinetic isotope effect (DKIE) by replacing hydrogens with deuteriums has emerged as a validated strategy to improve PK by blocking metabolic hotspots.[26-29] The strategic deployment of deuterium at sites of metabolism where the

cleavage of C-H is the rate determining step can impede metabolism and redirect metabolic pathways. This can often increase drug exposure and reduce drug toxicity.[29,30] However, deuterium replacement strategy may be confounded by metabolic switching and other metabolic pathways *in vivo*, for example deuterated Propofol and Imatinib.[31,32]

According to the metabolic profile of **5**, CYP2C8 and CYP3A4/5 (the major human cytochrome P450 isozymes) were responsible for the major metabolism of **5** to *N*-demethyl enzalutamide (M2).[33] To attenuate the *N*-demethylation pathway, hydrogen atoms of the *N*-methyl moiety were replaced by deuterium. We synthesized the *N*-methyl deuterated enzalutamide analogues and found that it has an improved PK profile and a better anti-tumor activity in animals.

Results and discussion

Chemistry

Enzalutamide **5**, and its deuterated version **6** were prepared as shown in Schemes 1. Key intermediates (**12** and **13**) were synthesized from commercially available 2-fluoro-4-nitrobenzoic acid (**7**). Starting from compound **7**, **12** and **13** were obtained via condensation with methylamine hydrochloride or methyl-d_3-amine hydrochloride (to **8** or **9**), reduction (to **10** or **11**), and a final Strecker reaction with ketone. Preparation of the target compounds **5** and **6** was finally achieved via cyclization. Aminoacetonitrile compound **12**, aniline **14** and thiophosgene ($CSCl_2$) were cyclized in *N*,*N*-Dimethylacetamide (DMAc) under 60 °C for 14h, followed addition of 2M HCl and ethanol, and refluxed for 2h, giving target product **5** in 41% yield. Under similar conditions, deuterated thiohydantoin **6** in 38% yield were produced through cyclization of compound **13** with **14** and $CSCl_2$ in DMAc under 60°C for 14h, and addition of 2M HCl and ethanol for reflux 2h.

In vitro proliferative and AR binding assays

The *in vitro* anti-proliferation activities were evaluated by using LNCaP/AR cells (prostate cancer cells overexpressing AR). In order to mimic the CRPC state, the cells were cultured in

charcoal stripped serum and treated with compounds for 6 days.[13] Cell viability was measured with the Cell Counting Kit-8. As expected, both compound **5** and **6** had similar anti-proliferation activities (data not shown). Meanwhile, the LNCaP/AR cells were used to study the affinity of **6** for AR by the competitive inhibition experiment. Both **6** and **5** inhibited the binding of [^{3}H] -R1881 (methyltrienolone) to AR with IC_{50} values of 0.58 ± 0.56 μM and 0.35 ± 0.24 μM, respectively. Due to the datum from three independent experiments, the SD (standard deviation) for the cell-based assay was very large.

Although there are measurable differences in physical chemical properties between hydrogen and deuterium,[29,34] they are too small to impact the *in vitro* biologic activities except metabolic stability of a deuterated drug. Particularly when only three H atoms of **5** have been replaced by D, **6** showed very similar inhibitory effects on prostate cancer cells and potency to bind to AR.

Pharmacokinetics study

PK properties of compounds **6** and **5** were assessed in male ICR mice with a single oral dose of 10 mg/kg (Figure 2A). As shown in Table 1, compound **6** exhibited an almost 2-fold increase in $t_{1/2}$ (24.7 h) compared to **5** (12.8 h); the $AUC_{0\text{-}24h}$ was also increased to 150.0 h·μg/ml (**6**) from 116.4 h·μg/ml (**5**), n=3.

Given the animal-to-animal variability, the deuterated compound **6** and non-deuterated analog **5** were co-administrated to male Balb/c mice (10/10 mg/kg), SD male rats (5/5 mg/kg), and male Beagle dogs (4/4 mg/kg) for side-by-side PK studies. All PK parameters in Table 2 were calculated based on the mean concentration vs time curves (Figure 2B, 2C, and 2D).

In mice, compound **6** exhibited increases in $t_{1/2}$ (12.5 h) and $AUC_{0\text{-}24h}$ (124 h·μg/ml) compared to **5** (11.0 h and 87.7 h·μg/ml). In rats, compound **6** had much better PK profiles than compound **5**, with ~1.5-fold increases in $t_{1/2}$ (18.3 vs 9.0 h) and ~1.5-fold increases in $AUC_{0\text{-}24h}$ (25.4 vs 17.0 h·μg/ml). In dogs, compound **6** also showed improvements in $t_{1/2}$ (41.6 h vs 34.5 h) and $AUC_{0\text{-}24h}$ (112.0 vs 96.6 h·μg/ml), compared to compound **5**. Overall, the *N*-methyl deuteration caused increases in $t_{1/2}$ and AUC, but had little, if any, effects on C_{max}

in these animals (Table 2). This suggests that at the same drug exposure compound **6** could have a reduction of C_{max}-driven toxicological effects.

In vivo efficacy studies using LNCaP/AR xenograft models of CRPC

SCID mice were castrated and subcutaneously inoculated with LNCaP-AR cells. When the tumor volumes reached 100-250 mm^3, the mice were randomly grouped (8 animals each group) and p.o. administrated with compound **6** or **5** at the doses of 1, 3, and 10 mg/kg, respectively, per day for 28 days. As shown in Figure 3A, except for 1 mg/kg of **5**, all other doses of **6** and **5** significantly inhibited the xenograft tumor growth in the SCID mice ($p<0.05$, compared with the vehicle group, by Kruskal Wallis Test). The values of tumor growth inhibition rate were summarized in Table 3. The changes in tumor volumes of the individual animal and body weight changes were summarized in Figure 3B and Figure 3C, respectively.

Collectively, it appears that at lower doses the tumor growth inhibition by **6** was more potent than **5**. The tumor suppression effect by **6** at 1 mg/kg was equivalent to that by **5** at 3 mg/kg (Figure 3A and 3B, Table 3). This could be caused by the improved pharmacokinetic property of **6** due to the 'deuteration effect' (the drug plasma concentrations shown in section 4.4). However, at dosage of 10 mg/kg/ **6** and **5** showed no differentiation in the anti-tumor activity, suggesting the dose saturation effect.

The drug concentrations in plasma, brain and tumor tissues following 28-day daily dosing

In the *in vivo* efficacy studies (section 4.3), 24 hours post last dosing, plasma, tumor and brain tissues were collected for the determination of parental drug and metabolites concentrations. As shown in Figure 3D, 3E and 3F, compound **6** had ~2-fold higher concentrations in the plasma, tumor, and brain tissues than compound **5** at the same dosages. This suggested that the stronger tumor suppression effect by **6** was indeed due to the elevated drug concentrations of **6** *in vivo*.

In our previous report, two major metabolites of **5** and **6** have been identified *in vivo*, oxidative metabolite *N*-demethyl enzalutamide (M2, active metabolite) and a carboxylic acid derivative

(M1) (Figure 1).[31] There were no differences in M1 concentrations of **6** and **5**. However, M2 concentrations of compound 6 were only 30-43% of compound **5**. These results suggest that blocking M2 production due to the 'deuteration effect' is one of the reasons for the elevated drug exposure of compound **6**. Though M2 could be the active metabolite, the concentrations of M2 in mice was quite low (Figure 3D, 3E and 3F) and its contribution to the *in vivo* efficacy should be limited.

Pharmacokinetic and pharmacodynamic (PK/PD) correlation analysis

In LNCaP/AR xenograft assay, the tumor proliferation rate of compound **6** at day 28 (last dosing) were graphed against the drug concentrations in the tumor tissues. As shown in Figure 4, in the dose range of 1, 3, and 10 mg/kg/day, **6**'s tumor suppression effect increased in the dose-dependent manner and was strongly correlated with the drug concentrations in the tumor tissue. In addition, as show in Figure 5, in the same dose range, the drug concentrations of **6** in the tumor tissue were strongly correlated with its concentrations in the plasma. These results suggest that the *in vivo* efficacy is reflected by the plasma drug concentrations.

Conclusion

The deuteration at *N*-methyl of **5** (primary metabolic site) had a better PK profile and stronger *in vivo* anti-tumor activity due to the elevated drug exposure in preclinical settings. Compound **6** is being developed clinically for the potential to be a best-in-class AR antagonist for the treatment of CRPC.

Experimental

Chemistry

Unless specified otherwise, starting materials and reagents were obtained from commercial sources and were used without further purification. Analytical TLC (thin-layer chromatography) was performed using 0.2mm silica gel plates (Yantai Jiangyou). And flash column chromatography was performed using silica gel with the indicated solvents. ^{1}H and ^{13}C NMR spectra were recorded on a Bruker 400 MHz instrument using $CDCl_3$, CD_3OD, or

DMSO-d_6 as the solvent and TMS as the internal reference. Chemical shifts (δ) were reported with parts per million (ppm) relative to the residual solvent peak (for $CDCl_3$, δ (^1H) = 7.26 ppm and δ (^{13}C) = 77.16 ppm; for CD_3OD, δ (^1H) = 3.31 ppm and δ (^{13}C) =49.00 ppm; and for DMSO-d_6, δ (^1H) = 2.50 ppm and δ (^{13}C) = 39.52 ppm). Abbreviations used for signal patterns are as follows: s, singlet; d, doublet; dd, doublet of doublets; ddd, doublet of doublet of doublets; t, triplet; q, quadruplet; m, multiplet; and br, broad. High-resolution mass spectrometry (HRMS) was performed with a Bruker micrOTOF-Q II (ESI) instrument. Liquid chromatography-Mass (LC/MS) were recorded on an Agilent LCMS 1200-6110 (ESI). All of the test compounds had purity >95% as determined by LC/MS.

*General procedure for preparation of the intermediates **12** and **13***

2-fluoro-*N*-trideuteriomethyl-4-nitrobenzamide (9). To a solution of 2-fluoro-4-nitrobenzoic acid (10.0g, 54.0mmol) and NEt_3 (16.4g, 162.2mmol) in DCM (100ml) was added CDI (10.5g, 64.9mmol) portion-wise under N_2 at room temperature. The reaction mixture was stirred for 1h. To this reaction mixture were added CD_3NH_2·HCl (5.7g, 81.1mmol), then the reaction mixture was stirred for 4h. After completion of the reaction water (100ml) was added. The organic layer was washed with 1M HCl (100ml) and water (100ml) orderly. The organic layer was dried over anhydrous sodium sulfate, and concentrated under reduced pressure. The residue was purified by flash column chromatography on silics gel (ethyl acetate/ petroleum ether=1/2) to afford 2-fluoro-*N*-trideuteriomethyl-4-nitrobenzamide (**9**) (10.3g, 95%). ^1H NMR (400 MHz, $CDCl_3$) δ 8.30 (dd, *J* = 8.6, 7.8 Hz, 1H), 8.13 (dd, *J* = 8.6, 2.1 Hz, 1H), 8.02 (dd, *J* = 11.1, 2.1 Hz, 1H), 6.79 (br, 1H). ^{13}C NMR (101 MHz, $CDCl_3$) δ 161.9, 159.7 (d, *J* =252.3Hz), 150.1 (d, *J* = 9.4 Hz), 133.4 (d, *J* = 2.7 Hz), 126.8 (d, *J* = 12.7 Hz), 119.7 (d, *J* = 3.6 Hz), 112.1 (d, *J* =30.7Hz), 26.5 (m). MS (ESI): m/z 201.7 ($M+H^+$, positive mode).

4-amino-2-fluoro-*N*-trideuteriomethylbenzamide (11). To a solution of compound **9** (10.0g, 49.8mmol) in EA (100ml) and AcOH (9.2ml, 0.50mol) was added Fe (13.9g, 249.0mmol) portion-wise under N_2 at room temperature. The reaction mixture was refluxed

for 16h. After cooling to room temperature, the reaction mixture was filter, then the filtrate was concentrated under reduced pressure. The residue was purified by flash column chromatography on silics gel (EA/PE=1/1) to afford 4-amino-2-fluoro-*N*-trideuteriomethylbenzamide (**11**) (5.9g, 69%). ^{1}H NMR (400 MHz, $CDCl_3$) δ 7.89 (t, *J* = 8.6 Hz, 1H), 6.61 (d, *J* = 12.2 Hz, 1H), 6.48 (dd, *J* = 8.6, 2.2 Hz, 1H), 6.33 (dd, *J* = 14.4, 2.2 Hz, 1H), 4.15 (br, 2H). ^{13}C NMR (101 MHz, $CDCl_3$) δ 164.4, 162.2 (d, *J* =245.7Hz), 151.5 (d, *J* = 12.8 Hz), 133.3 (d, *J* = 4.3 Hz), 110.9 (d, *J* = 1.8 Hz), 110.2 (d, *J* = 11.9 Hz), 100.8 (d, *J* =28.8Hz), 25.8 (m). MS (ESI): m/z 172.2 ($M+H^+$, positive mode).

4-((2-cyanopropan-2-yl)-amino)-2-fluoro-*N*-trideuteriomethylbenzamide (13). In a sealed tube with a magnetic stir bar, compound **11** (171mg, 1.0 mmol) was added, followed by TMSCN (298mg, 3.0mmol), acetone (5ml) and AcOH (5ml). The sealed tube was heated to 80°C and stirred for 16h. After cooling to room temperature, EA (20ml) was added and then washed with water (20ml). The organic layer was dried over anhydrous sodium sulfate, and concentrated under reduced pressure. The residue was purified by flash column chromatography on silics gel (EA/PE=1/2) to afford 4-((2-cyanopropan-2-yl)amino)-2-fluoro-*N*-trideuteriomethylbenzamide (**13**) (217mg, 90%). ^{1}H NMR (400 MHz, $CDCl_3$) δ 7.79 (t, *J* = 8.7 Hz, 1H), 7.06 (d, *J* = 10.3 Hz, 1H), 6.70 (dd, *J* = 8.7, 2.3 Hz, 1H), 6.59 (dd, *J* = 14.7, 2.2 Hz, 1H), 6.41 (br, 1H), 1.72 (s, 6H). ^{13}C NMR (101 MHz, $CDCl_3$) δ 164.2, 161.4 (d, *J* = 246.1Hz), 149.3 (d, *J* = 12.0 Hz), 132.1 (d, *J* = 4.3 Hz), 121.4, 110.8, 110.7 (d, *J* = 13.2 Hz), 100.7 (d, *J* = 29.3 Hz), 47.6, 27.5, 25.8 (m). MS (ESI): m/z 239.3 ($M+H^+$, positive mode).

*General procedure for preparation of compounds **5** and **6**.*

To a solution of compound **12** (235mg, 1.0mmol) and compound **7** (223mg, 1.2mmol) in DMA (0.5ml) was added thiophosgene (172mg, 1.5mmol) under N_2 at 0°C. The reaction mixture was stirred for 16h at 60°C. To this mixture were added MeOH (2ml) and 2M HCl (2ml), then the reaction mixture was reflux for 2h. After cooling to room temperature, the reaction mixture was poured into ice water (10ml) and extracted with EA (10ml). The organic

layer was dried over anhydrous sodium sulfate, and concentrated under reduced pressure. The residue was purified by flash column chromatography on silics gel (EA/ PE=1/1) to afford 4-(3-(4-cyano-3-(trifluoromethyl)phenyl)-5,5-dimethyl-4-oxo-2-thioxoimidazolidin-1-yl)-2-fluoro-*N*-methylbenzamide (**5**) (190mg, 41%).

4-(3-(4-cyano-3-(trifluoromethyl)phenyl)-5,5-dimethyl-4-oxo-2-thioxoimidazolidin-1-yl)-2-fluoro-*N*-methylbenzamide (enzalutaimde, 5). White solid; yield: 41 %; ^{1}H NMR (400 MHz, DMSO-d_6): δ 8.44 (dd, *J* = 20.7, 5.8 Hz, 2H), 8.30 (s, 1H), 8.09 (d, *J* = 8.1 Hz, 1H), 7.79 (t, *J* = 8.0 Hz, 1H), 7.44 (d, *J* = 10.6 Hz, 1H), 7.34 (d, *J* = 8.1 Hz, 1H), 2.80 (d, *J* = 4.2 Hz, 3H), 1.55 (s, 6H). ^{13}C NMR (100 MHz, DMSO-d_6): δ 180.04, 174.70, 163.42, 158.90 (d, *J* = 251.49Hz), 138.24(d, *J* = 10.1Hz), 137.88, 136.22, 133.91，131.12(q, *J* = 33.33Hz), 130.85(d, *J* = 4.04Hz), 127.95(q, *J* = 4.04Hz), 126.08 (d, *J* = 3.03Hz), 125.12 (d, *J* = 15.15Hz), 122.17(q, *J* =274.72Hz), 118 (d, *J* = 24.24Hz), 114.97, 108.71 (d, *J* =2.02Hz), 66.55, 25.54, 22.89. MS (ESI): m/z 465.2 ($M+H^+$, positive mode). HRMS (ESI): mass calcd for $C_{21}H_{17}F_4N_4O_2S$ ($M+H^+$, positive mode), 465.1008; found, 465.1028.

4-(3-(4-cyano-3-(trifluoromethyl)phenyl)-5,5-dimethyl-4-oxo-2-thioxoimidazolidin-1-yl)-2-fluoro-*N*-trideuteriomethylbenzamide (6). White solid; yield: 39%; ^{1}H NMR (400 MHz, DMSO-d_6) δ 8.50-8.36 (m, 2H), 8.30 (s, 1H), 8.09 (d, *J* = 8.1 Hz, 1H), 7.79 (s, 1H), 7.44 (d, *J* = 10.5 Hz, 1H), 7.34 (d, *J* = 8.2 Hz, 1H), 1.54 (s, 6H). ^{13}C NMR (100 MHz, DMSO-d_6): δ 180.04, 174.70, 163.42, 158.90 (d, *J* = 251.5Hz), 138.24(d, *J* = 10.1Hz), 137.88, 136.22, 133.91, 131.12(q, *J* = 33.3Hz), 130.85(d, *J* = 4.0Hz), 127.95(q, *J* = 4.0Hz), 126.08 (d, *J* = 3.0Hz), 125.12 (d, *J* = 15.2Hz), 122.17(q, *J* =274.7Hz), 118 (d, *J* = 24.2Hz), 114.97, 108.71 (d, *J* =2.0Hz), 66.55, 25.54 (m, *J* = 21.2Hz), 22.89. MS (ESI): m/z 468.2 ($M+H^+$, positive mode). HRMS (ESI): mass calcd for $C_{21}H_{14}D_3F_4N_4O_2S$ ($M+H^+$, positive mode), 468.1197; found, 468.1191.

Bioassay

Animals and cells

ICR mice (males, 23-33 g) and SD rats (males, 180-220 g) were purchased from Shanghai Lingchang biological technology co., LTD, (Shanghai, China). CB17 SCID mice (males, 4-5 weeks old, 18-22 g) were purchased from Beijing HFK Bioscience co., LTD. (Beijing, China). Beagle dogs (males, 6-9 monthes old, 6-9 kg) were purchased from Beijing Marshall Biotechnology Co., LTD. (Beijing, China). LNCaP/AR cell lines were obtained from Sichuan University and Collaborative Innovation Center for Biotherapy (Chengdu, China).

All animals were kept in an animal room with controlled illumination (12/12 h light/dark cycle), temperature (20-25°C), and humidity (over 40 %). The animals were fasted for 12 h before dose administration. All PK studies were performed at Shanghai Institute of Materia Medica (Chinese Academy of Sciences), and all *in vitro* and *in vivo* biologic activity studies performed at Sichuan Kangcheng biological co., LTD. The animal studies were carried out under protocols approved by the animal protection law of the People's Republic of China Care and Use Committees and institutional guidelines for the proper, humane use of animals. All rodent studies were also carried out in accordance with the Guidelines for Care and Use of Laboratory Animals approved by the Shanghai Institute of Materia Medica, Chinese Academy of Sciences (Shanghai, China).

Proliferation assays

Trypsinized LNCaP/AR cells were adjusted to a concentration of 60,000 cells per mL in RPMI 1640 (with 5% CSS), and dispensed in 100 μl aliquots into 96 well plates (Corning). Cells were cultured for 24 h and then 100 μl of culture medium containing compounds were added. The cells continued to incubate for 6 days and the cell viability was measured using the Cell Counting Kit-8 (Dojindo) according to the manufacturer's instructions. Percent inhibition of the samples was calculated as follows: %inhibition= [$OD_{\text{value of control cells}}$ - $OD_{\text{value of sample treated cells}}$]/[$OD_{\text{value of control cells}}$- $OD_{\text{value medium without cells}}$]. The IC_{50} values were calculated by using the Prism Graph software.

AR binding assays

The LNCap/AR cells were cultured with RPMI1640 plus 10% FBS at 37°C, 5% CO_2. 6×10^4 cells were added to the 96-well plate (Poly-D pre-coated), and incubated for overnight. The medium was removed, then, 25μl compound dose (top concentration: 200 μM, three-fold dilution) was added. Firstly, the cells were incubated for 30 min, then 25μM [^{3}H]-R1881 (final top concentration is 100μM, three-fold dilution, final [^{3}H]-R1881 concentration is 7nM) was added, the cells were incubated for 30 min again. The medium was removed, then the cells were washed with uptake buffer (10mM HEPEs, pH 7.5, 125mM NaCl, 4.8mM KCl, 1.2mM $CaCl_2$, 1.2mM MgSO4, 1.2mM KH_2PO4, 5.6mM D-Glucose), and 100μl lysis buffer was added. Shaking the plate for 1 hour, the 50μl lysis buffer was transfered to an isotope plate, 200μl scintillation cocktail was added, and the dates were counted on the MicroBeta.

Single-dosing ICR mice, SD rat, and Beagle dogs PK study

The **5** and **6** were dissolved in 0.5% HPMC at a concentration of 1 mg/ml. A total of nine male ICR mice were randomly divided into three groups (A group, four rats; B group, four rats; C group, three rats). The A and B groups were orally given 10 mg/kg **5** and **6**, respectively. The blood sampling time points were pre-dose (0) and 0.5, 1, 2, 4, 6 and 24 h post-doses. Group C was given a 1:1 formulation of **5** and **6** (10/10 mg/kg) by oral administration. The blood sampling time points were pre-dose (0) and 0.25, 0.5, 1, 2, 3, 5, 7, 9, 24, 32 and 48 h post-doses. Four male SD rats were given a 1:1 formulation of **5** and **6** (5/5 mg/kg) by oral administration. The blood sampling time points were pre-dose (0) and 0.5, 1, 3, 5, 7, 9, 24, 48, 72, 96 and 120 h post-doses. Three-hundred microliters of blood was collected from the orbital plexus into tubes after these animals were temporarily anesthetized by ether inhalation. Three Beagle dogs were given a 1:1 formulation of **5** and **6** (4/4 mg/kg) by oral administration. The blood sampling time points were pre-dose (0) and 0.5, 1, 2, 3, 4, 6, 8, 12, 24, 48, 96, 114, 192, 240, 288 and 336 h post-doses. One milliliter of blood was collected from the upper arm cephalic vein into tubes. Immediately after collection, blood collection tubes were gently inverted at least five times, ensuring complete mixing, and were

then immediately placed on ice. The blood was centrifuged for 10 min at 3500 rpm and 4°C to separate the plasma from the red blood cells. After separation, 200μl disposable pipettes were used to take 100μl aliquots from the top plasma layer into tubes, with each being labeled by the name of analysis unit. Plasma was stored at −20 °C until removal for LC-MS/MS analysis for the test compound concentration.

In vivo LNCaP/AR xenograft experiments.

In vivo xenograft experiments to determine anti-tumor response were carried out in CB17 SCID male mice. Mice were orchiectomized under pentobarbital sodium and were given 2-3 days to recover prior to tumor cell injection. LNCaP/AR cells were suspended in 50% RPMI, 50% Matrigel, and 1×10^7 cells/xenograft were injected in a volume of 100μl. Animals were observed 3 times/week until tumor growth was apparent. From 21 day post-injection, tumors were measured weekly, and after 40-60 days post-injection, animals were randomized into cohorts of equivalent mean (100-250 mm^3) and range tumor burden. The **5** and **6** were administered daily by oral gavage at the dose of 1, 3, and 10 mg/kg/d, respectively. For all LNCaP/AR xenograft studies **5** and **6** drug stocks were prepared in 18% PEG-400, 1% Tween-80 and 1% povidone, and were formulated for dosing in 15% Vitamin E-TPGS and 65% of a 0.5% w/v CMC solution in 20mM citrate buffer (pH 4.0).

The blood sample, tumor tissue, and brain were collected 24 hours later after the last administration, sequentially. The blood samples were added EDTA, and the samples were stored at -20 °C for LC-MS/MS analysis after being thoroughly vortexed. The tumor tissue and brain were accurately weighed and taken photos, then were stored at -20 °C for LC-MS/MS analysis.

Acknowledgments

This work is financially supported by Hinova Pharmaceuticals Inc. and also partially supported by National Natural Science Foundation of China (No. 81472418). We also thank Prof. Xiaoyan Chen, and Prof. Zhiwei Gao (Shanghai Institute of Materia Medica, Chinese Academy of Sciences) for the technical support of Pharmacokinetic experiments.

Conflict of Interest

The authors have declared that there is no conflict of interest.

References

1. Baade PD, Youlden DR, Krnjacki LJ. International epidemiology of prostate cancer: geographical distribution and secular trends. *Molecular nutrition & food research.* **2009**;53(2):171-184.
2. McConnell JD. Physiological basis of endocrine therapy for prostatic cancer. *Urol. Clin. North Am.* **1991**;18:1-13.
3. Handratta VD, Vasaitis TS, Njar VCO, et al. Novel C-17-Heteroaryl Steroidal CYP17 InhibitorsAntiandrogens Synthesis, in Vitro Biological Activity, Pharmacokinetics, and Antitumor Activity in the LAPC4 Human Prostate Cancer Xenograft Model. *J. Med. Chem.* **2005**;48:2972-2984.
4. Njar VC, Brodie AM. Discovery and development of Galeterone (TOK-001 or VN/124-1) for the treatment of all stages of prostate cancer. *Journal of medicinal chemistry.* **2015**;58(5):2077-2087.
5. Denis L. Role of maximal androgen blockade in advanced prostate cancer. . *Prostate cancer.* **1994**;5(Suppl.):17-22.
6. Crawford ED, Allen JA. Treatment of newly diagnosed state D2 prostate cancer with leuprolide and flutamide or leuprolide alone, Phase III: intergroup study 0036. *J. Urol.* **1992**;147: 417.
7. Crawford ED, Eisenberger MA, McLeod DG, et al. A controlled trial of leuprolide with and without flutamide in prostatic carcinoma. *N. Engl. J. Med.* **1989**;321:419-424.
8. Courtney KD, Taplin ME. The evolving paradigm of second-line hormonal therapy options for castration-resistant prostate cancer. *Current opinion in oncology.* **2012**;24(3):272-277.
9. Yap TA, Zivi A, Omlin A, de Bono JS. The changing therapeutic landscape of

castration-resistant prostate cancer. *Nat. Rev. Clin. Oncol.* **2011**;8:597-610.

10. Taplin ME. Androgen receptor: role and novel therapeutic prospects in prostate cancer. *Expert Rev. Anticancer Ther.* **2008**;8:1495-1508.
11. Chen Y, Sawyers CL, Scher HI. Targeting the androgen receptor pathway in prostate cancer. *Current opinion in pharmacology.* **2008**;8(4):440-448.
12. Feldman BJ, Feldman D. The development of androgen-independent prostate cancer. *Nat. Rev. Cancer.* **2001**;1:34-45.
13. Chen CD, Welsbie DS, Tran C, et al. Molecular determinants of resistance to antiandrogen therapy. *Nature medicine.* **2004**;10(1):33-39.
14. Linja MJ, Savinainen KJ, Saramaki OR, Tammela TL, Vessella RL, Visakorpi T. Amplification and overexpression of androgen receptor gene in hormone-refractory prostate cancer. *Cancer Res.* **2001**;61:3550-3555.
15. Gregory CW, Johnson RTJ, Mohler JL, French FS, Wilson EM. Androgen receptor stabilization in recurrent prostate cancer is associated with hypersensitivity to low androgen. *Cancer research.* **2001**; 61:2892-2898.
16. Koivisto P, Visakorpi T, Kallioniemi OP. Androgen receptor gene amplification: a novel molecular mechanism for endocrine therapy resistance in human prostate cancer. *Scand J Clin Lab Invest Suppl.* **1996**; 226:57-64.
17. Knudsen KE, Penning TM. Partners in crime: deregulation of AR activity and androgen synthesis in prostate cancer. *Trends in endocrinology and metabolism: TEM.* **2010**;21(5):315-324.
18. Scher HI, Sawyers CL. Biology of progressive, castration-resistant prostate cancer: directed therapies targeting the androgen-receptor signaling axis. *Journal of clinical oncology : official journal of the American Society of Clinical Oncology.* **2005**;23(32):8253-8261.
19. Attard G, Cooper CS, de Bono JS. Steroid hormone receptors in prostate cancer: a hard habit to break? *Cancer cell.* **2009**;16(6):458-462.
20. Hara T, Miyazaki J, Araki H, et al. Novel mutations of androgen receptor: a possible

mechanism of bicalutamide withdrawal syndrome. *Cancer research.* **2003**;63:149–153.

21. Taplin ME, Bubley GJ, Ko YJ, et al. Selection for androgen receptor mutations in prostate cancers treated with androgen antagonist. *Cancer research.* **1999**;59: 2511-2515.
22. Tran C, Ouk S, Clegg NJ. Development of a second-generation antiandrogen for treatment of advanced prostate cancer. *Science.* **2009**;324(5928):787-790.
23. Jung ME, Ouk S, Yoo D, et al. Structure-activity relationship for thiohydantoin androgen receptor antagonists for castration-resistant prostate cancer (CRPC). *Journal of medicinal chemistry.* **2010**;53(7):2779-2796.
24. Sanford M. Enzalutamide: a review of its use in metastatic, castration-resistant prostate cancer. *Drugs.* **2013**;73(15):1723-1732.
25. Scher HI, Fizazi K, Saad F, et al. Increased survival with enzalutamide in prostate cancer after chemotherapy. *The new england journal of medicine.* **2012**;367(13):1187-1197.
26. Xu G, Lv B, Roberge JY, et al. Design, synthesis, and biological evaluation of deuterated C-aryl glycoside as a potent and long-acting renal sodium-dependent glucose cotransporter 2 inhibitor for the treatment of type 2 diabetes. *Journal of medicinal chemistry.* **2014**;57(4):1236-1251.
27. Harbeson SL, Tung RD. Deuterium Medicinal Chemistry-A New Approach to Drug Discovery and Development. *Medchem news.* **2014**;2:8-22.
28. Sharma R, Strelevitz TJ, Gao H, et al. Deuterium isotope effects on drug pharmacokinetics. I. System-dependent effects of specific deuteration with aldehyde oxidase cleared drugs. *Drug metabolism and disposition: the biological fate of chemicals.* **2012**;40(3):625-634.
29. Meanwell NA. Synopsis of some recent tactical application of bioisosteres in drug design. *Journal of medicinal chemistry.* **2011**;54(8):2529-2591.
30. NELSON SD, TRAGER WF. The use of deuterium isotope effects to probe the active

site properties, mechanism of cytochrome P450-catalyzed reactions, and mechanisms of metabolically dependent toxicity. *Drug metabolism and disposition.* **2003**;31:1481-1498.

31. Jiang J, Pang X, Li L, et al. Effect of N-methyl deuteration on metabolism and pharmacokinetics of enzalutamide. *Drug design, development and therapy.* **2016**;10:2181-2191.

32. Helfenbein J, Lartigue C, Noirault E, et al. Isotopic Effect Study of Propofol Deuteration on the Metabolism, Activity, and Toxicity of the Anesthetic. *J. Med. Chem.* **2002**; 45:5806-5808.

33. Gibbons JA, Ouatas T, Krauwinkel W, et al. Clinical Pharmacokinetic Studies of Enzalutamide. *Clinical pharmacokinetics.* **2015**;54(10):1043-1055.

34. El Tayar N, van de Waterbeemd H, Gryllaki M, Testa B, Trager WF. The lipophilicity of deuterium atoms. A comparison of shakeflask and HPLC methods. *Int. J. Pharm.* **1984**;19:271-281.

Table 1. Pharmacokinetic parameters orally respective administration of **6** and **5**.[a]

Compound	Dose (mg/kg)	T_{max} (h)	C_{max} (μg/ml)	$AUC_{0\text{-}24h}$ (h·μg/ml)	$t_{1/2}$ (h)
5	10	5.0	5.35±0.32	116.4±4.2	12.8±0.9
6	10	4.0	4.13±0.54	150.0±21.3	24.7±3.9

[a]Data are presented as the mean of values obtained from three ICR mice.

Table 2. Pharmacokinetic parameters of PO combination dosing of compounds **5** and **6.** [a]

Animal	Compound	Dose (mg/kg)	T_{max} (h)	C_{max} (μg/ml)	$AUC_{0\text{-}24h}$ (h·μg/ml)	$t_{1/2}$ (h)
Mouse	**5**	10	5.0	5.48	87.7	11.0
	6	10	5.0	5.97	124	12.5
Rat	**5**	5	6.0	0.9	17.0	9.0
	6	5	6.0	0.87	25.4	18.3
Dog	**5**	4	2.0	4.13	96.6	34.5
	6	4	2.0	4.25	112.0	41.6

[a]Data are presented as the mean of values obtained from three animals.

Table 3. Tumor weight and inhibitory rate.[a]

Group	Dose (mg/kg)	n	Tumor weight (g)	Inhibitory rate (%)
Vehicle	-	10	0.199±0.028	0.00
5	10	8	0.049±0.010*	75.49
	3	8	0.094±0.030**	50.73
	1	8	0.149±0.032	25.40
6	10	8	0.039±0.005**	80.57
	3	8	0.062±0.014**	68.72
	1	7▲	0.082±0.008**	58.73

[a]Each value represents the mean ± SEM. ▲ One animal died after grouping; * P<0.05，** P<0.01.

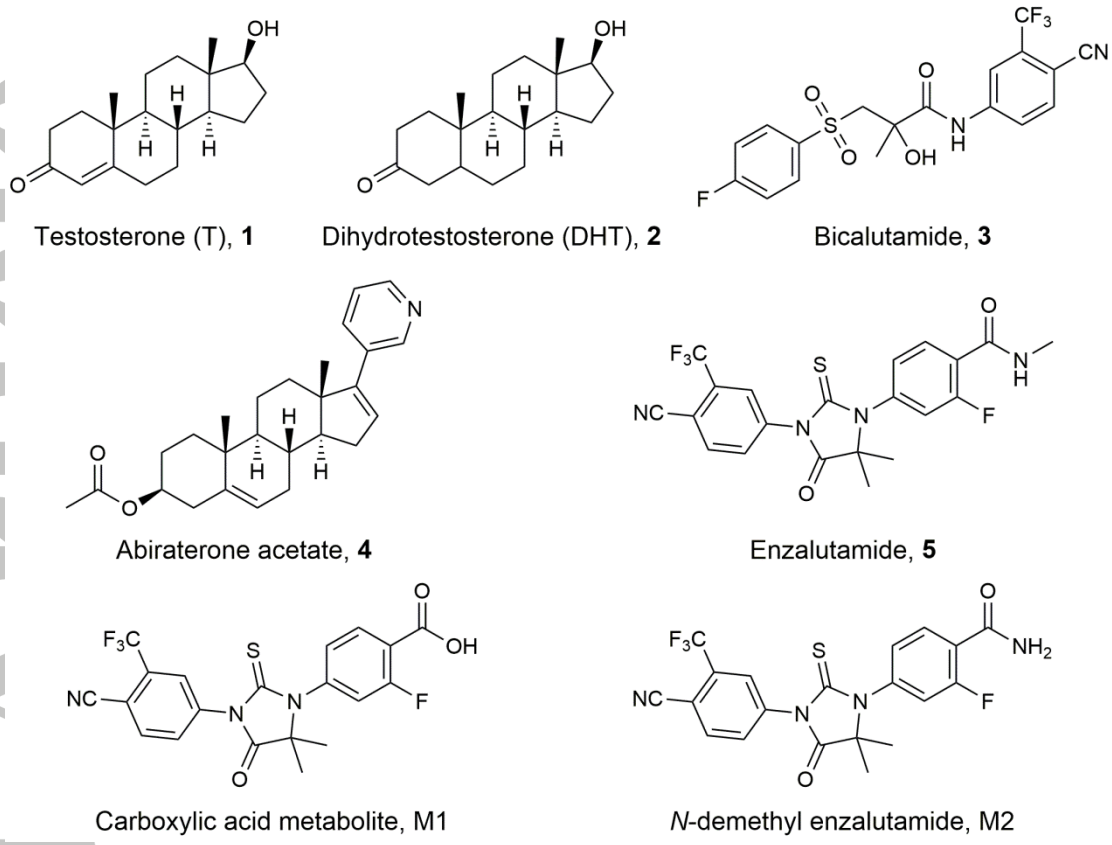

Figure 1. Structures of androgens (**1** and **2**), antiandrogens (**3** and **5**), inhibitor of CYP17A1 (**4**), and metabolites of enzalutamide (M1 and M2).

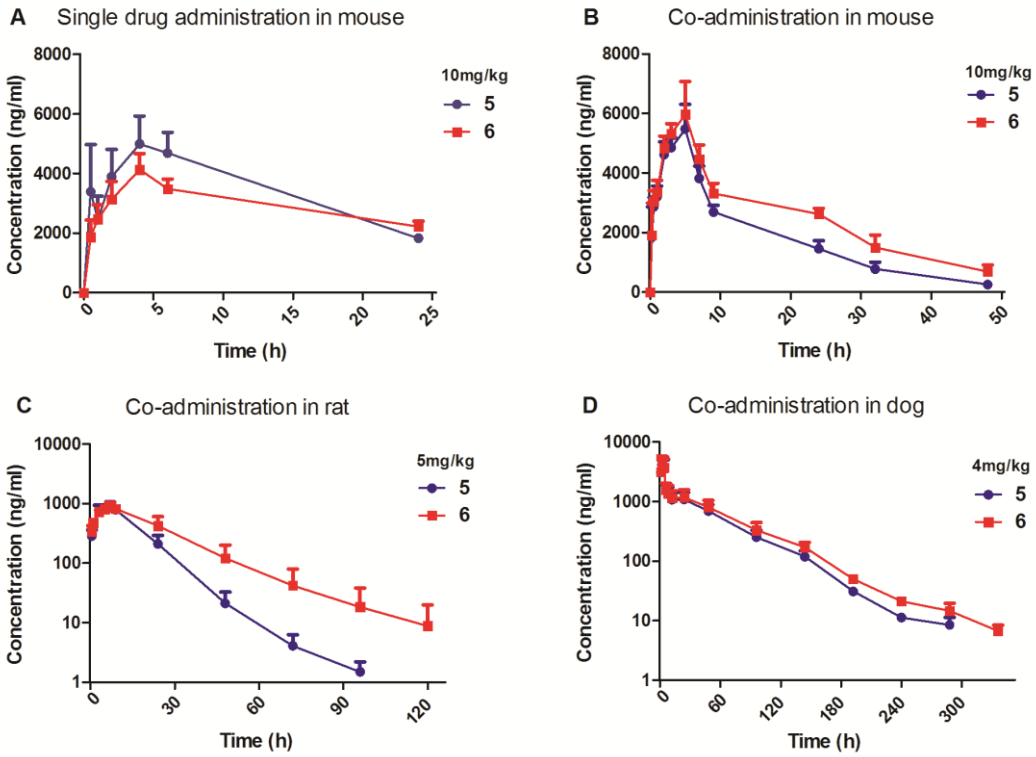

Figure 2. The concentration of **5** and **6** in plasma. A, Orally respective administration of **6** and **5** in mice; B, Orally co-administration of **6** and **5** in mice; C, Orally co-administration of **6** and **5** in rats; D, Orally coadministration of **6** and **5** in dogs.

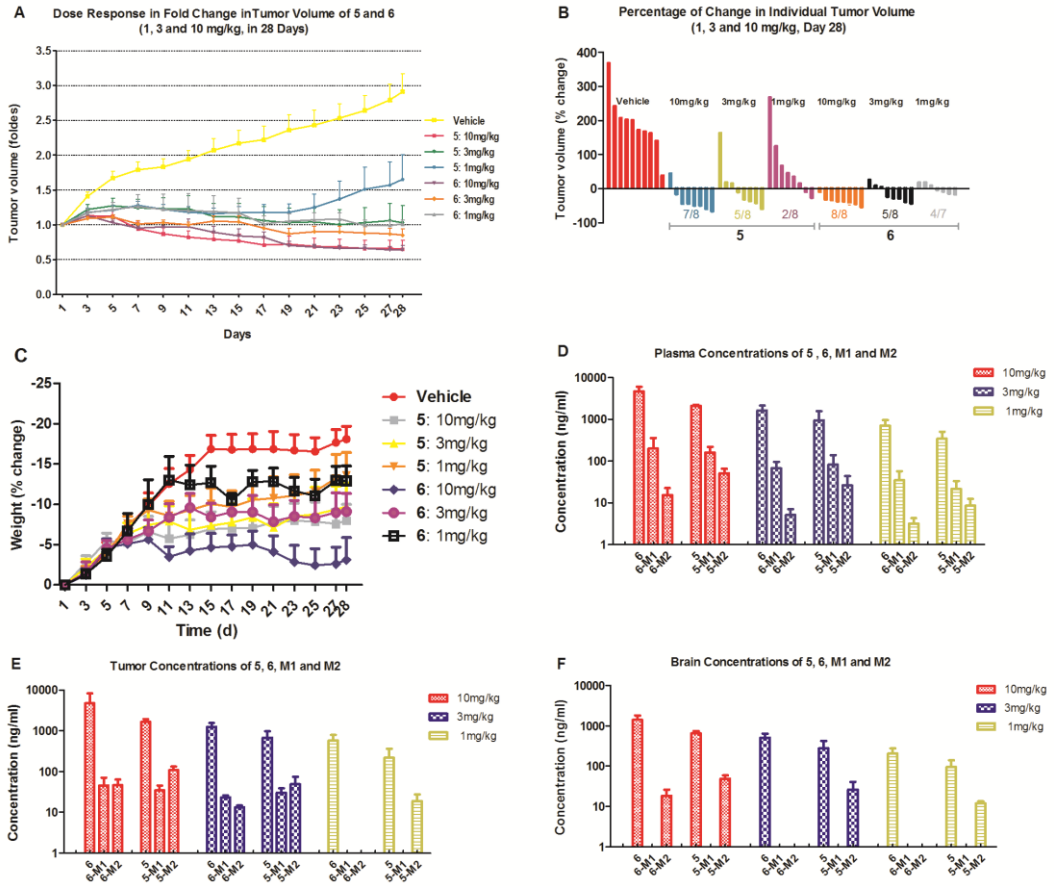

Figure 3. A, The fold change in tumor volume of xenografts with **5** and **6** in 28 days; B, The percentage of change in individual tumor volume; C, The weight fold change of tumor-burdened mice in 28 days; D, The concentration of **5**, **6**, and major metabolites (M1 and M2) in plasma 24 h post last dosing after 28-day dosing; E, The concentration of **5**, **6**, M1 and M2 in tumor; F, The concentration of **5**, **6**, M1 and M2 in brain.

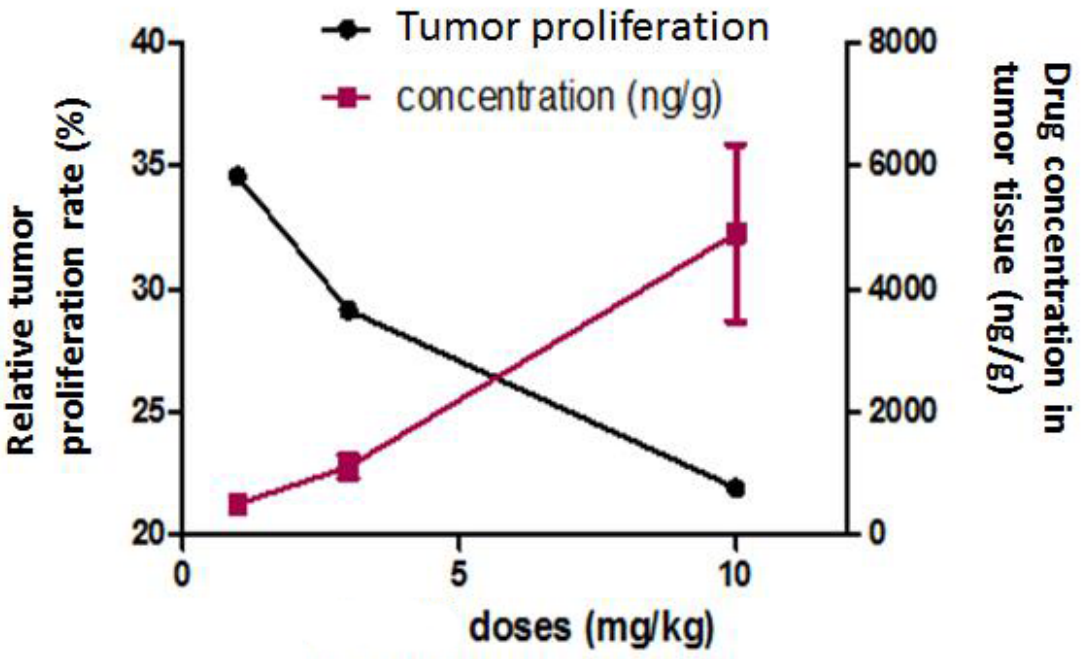

Figure 4. The tumor suppression effect of **6** correlating with its concentrations in the tumor tissue.

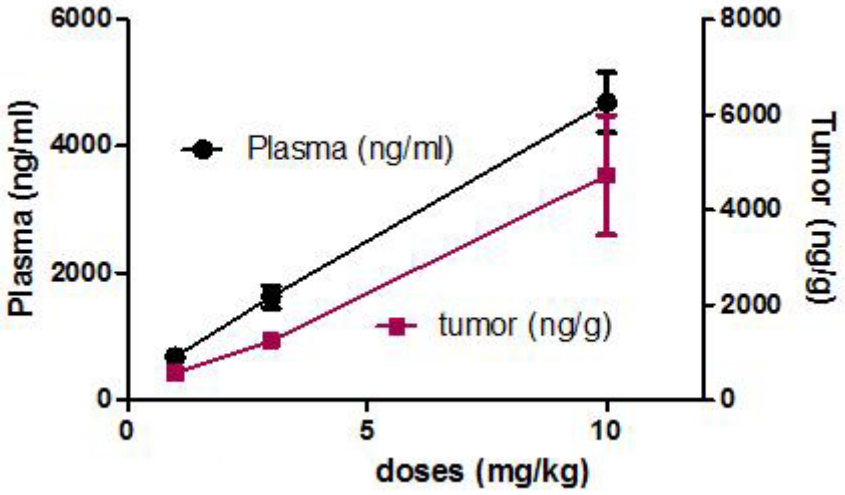

Figure 5. The concentrations of **6** in the tumor tissue correlating with its concentrations in the plasma.

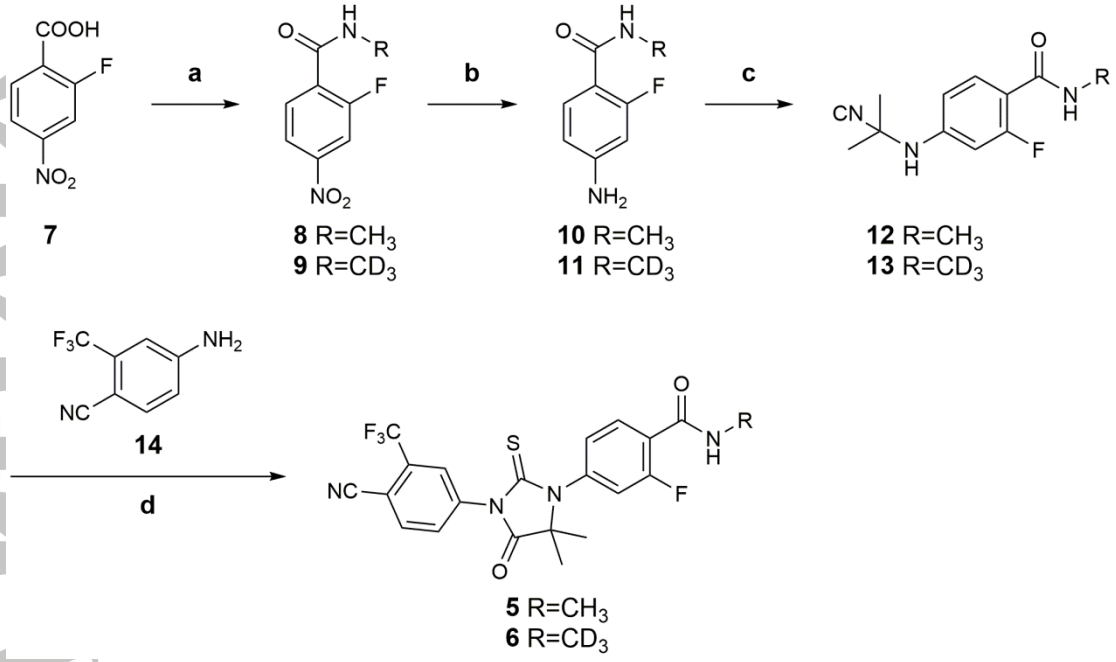

Scheme 1. Synthesis of **5** and **6**. Reagents and conditions: (a) $MeNH_2 \cdot HCl$ or $CD_3NH_2 \cdot HCl$, CDI, NEt_3, DCM, 3h, 93-95%; (b) Fe, AcOH, EA, reflux, 16h, 69-73%; (c) TMSCN, AcOH, Acetone, sealed tube, 80°C, 16h, 76-90%; (d) $CSCl_2$, DMA, 60°C, 16 h, then 2M HCl, EtOH, reflux, 2h, 38-41%.